Preprint of http://dx.doi.org/10.1016/j.proci.2008.05.034

Peel-Off Case Failure in Thermal Explosions Observed by the Deflagration Cylinder Test

L. G. Hill [a], J. S. Morris [a], S. I. Jackson [a]

[a] *Los Alamos National Laboratory, Los Alamos, NM 87545 USA*

Contact: Larry Hill
Mail Stop P952
Los Alamos National Laboratory
Los Alamos, NM 87545 USA
FAX: (505) 667-6372
Email: lgh@lanl.gov

Colloquium: 80.00 Detonations, Explosions, and Supersonic Combustion

Total Length: 6180 words by Method 1
Word Equivalent Length Breakdown:
Main Text: 4318
Equations: 213
References: 318
Table 1: 76
Fig. 1 103
Fig. 2: 153
Fig. 3: 78
Fig. 4: 120
Fig. 5: 72
Fig. 6: 128
Fig. 7: 122
Fig. 8: 102
Fig. 9: 121
Fig. 10: 121
Fig. 11: 135

Color: I agree to pay color charges if applicable.

Preprint of http://dx.doi.org/10.1016/j.proci.2008.05.034

Abstract

We have discovered a previously unidentified thermal explosion mode using the Los Alamos *deflagration cylinder test* (DFCT). The DFCT is a "pipe bomb"-style test similar to the *detonation cylinder test* (DTCT), which has been used for many years to calibrate detonation product equations of state. The shot is heated in an oven to a uniform test temperature. The pre-heated high explosive (HE) is triggered by a hot wire initiator on one end. The tube is back-illuminated by a bright light source, and its combustion-driven deformation and subsequent break-up are observed by a high-speed framing camera. Like the DTCT, the DFCT tube wall motion provides the primary diagnostic. A variety of reactive responses are possible, including quasi-steady deflagration and deflagration-to-detonation transition. This paper focuses on the behavior of the HMX-based explosive PBX 9501 at 155 C. Under this condition burning appeared to occur only at the HE/tube interface, causing the tube to peel away from the HE core. Peel-off propagated as a wave that traveled along the tube at ∼500 m/s. This failure mode resulted in vigorous case venting, but the response was otherwise benign. We derive a steady peel-off-wave model that reproduces the essential observed features for realistic PBX 9501 parameter values.

Key words: Deflagration, High explosive, Thermal explosion, Cookoff, Cylinder test

Email addresses: lgh@lanl.gov (L. G. Hill), jsmorris@lanl.gov (J. S. Morris), sjackson@lanl.gov (S. I. Jackson).

Preprint of http://dx.doi.org/10.1016/j.proci.2008.05.034

1 Introduction to HE Thermal Safety

The thermal response of high explosive (HE) systems is a complex, interesting, and important problem. It is complex and interesting because it depends sensitively on many parameters of the HE material, thermal environment, and system configuration. It is important because it comprises one of the main HE hazards with respect to personnel and materiel.

HE thermal safety research surely benefits from engineering tests that would seek to mock presenting hazards. However, since reactive response is sensitive to many parameters, the behavior of lab-scale tests designed to mimic aspects of a real system will not necessarily behave like the real item. Consequently, engineering models calibrated from lab data may not faithfully simulate the real system.

Physically-based models motivated by observed phenomenology have the best chance of predicting a wide range of scenarios; however, such descriptions are a long way off. As such, a good strategy is to devise tests that provide both engineering and physical data, so as to work both short and long term problems in parallel. The *deflagration cylinder test* (DFCT) is such a test.

2 Deflagration Cylinder Test

The DFCT concept is motivated by the success of the *detonation cylinder test* (DTCT), which for the past 40+ years has been used to calibrate the Jones-Wilkins-Lee (JWL) detonation product equation of state (EOS) for high explosives. The DFCT and DTCT are both instrumented, precision pipe bombs in which an HE-filled copper tube is initiated at one end. The DTCT, a performance test, is typically fired at room temperature by detonating the HE. The DFCT, a thermal safety test, is typically fired at a uniform elevated initial tem-

perature close to the HE critical temperature, and is either hot-wire-ignited or possibly cooked to auto-ignition.

The first goal of the DFCT is to explore the range of cookoff explosion behavior for tubular systems with moderate ductile confinement. The second goal is to deduce the essential physical mechanisms, and to develop simple phenomenological models to help elucidate them. The third goal, discussed in more detail elsewhere [4], is to formulate engineering descriptions of the post-ignition response. The strategy is to determine—so far as the behavior allows—equation-of-state-like descriptions of the deflagrating flows, which one hopes will be at least modestly transferable to other configurations.

Deflagration to detonation transition (DDT) tubes have been used to study gas phase detonations for many years. Similar tests have been developed to study DDT in condensed phase explosives, e.g., [1][2]. Our DFCT belongs to that genre; however, the use of wall motion to explicitly deduce the internal flow structure represents a new twist on the old theme. The DFCT test has undergone minor evolutionary design changes since its inception; the following description applies to the current variant.

The nominal DFCT dimensions are taken from the standard DTCT. The copper tube is 1-in (25.4 mm) i.d., 1.2-in (30.48 mm) o.d., and 12-in (304.8 mm) long. Likewise the tube material and its preparation are the same for both tests: alloy C101 copper (99.99% pure), annealed to dead soft temper. Like the DTCT, we wish the DFCT tube to stretch as much as possible before rupturing. The test is over when the tube first splits, at least so far as simple data analysis is concerned. Consequently, neither test variant may have any holes drilled through the tube to pass instrumentation, nor any substantial

obstructions around the tube.

Unlike the DTCT, the DFCT must maintain a gas-tight seal throughout the course of the experiment. This is because confinement is necessary in order to achieve violent reaction in the thermally-initiated test explosive PBX 9501 (95 wt % HMX, 5 wt % binder). In fact, unless deflagration to detonation transition (DDT) has occurred prior to that point, even well-established burning has a tendency to attenuate when confinement fails. Consequently, the tube is plugged and sealed on both ends, such that the tube wall fails before the end seals do.

Figure 1 shows a scale drawing of the test assembly. The hot wire leads pass through the left end plug, and four thermocouple wires pass through the right end plug. All wires are sealed by high-pressure feedthroughs. The triangular steel end plates are connected at their vertices by three stainless steel support rods, the purpose of which is to fix the end plate distance during cookoff. Without this constraint, the tube length contracts as the width expands, complicating the analysis. The stainless steel thermal expansion coefficient is virtually the same as for the copper, such that the rods induce very little stress in the tube during heating. A fringe benefit is that the rods make effective witness bars in the event of a violent reaction leading to DDT.

The HE is inserted into the tube in close-fitting 1-in (25.4 mm) long segments. Counterbores machined on one end of each segment provide ullage to accommodate the greater HE thermal expansion relative to the copper. For initial temperatures at which the HMX has transitioned to the δ-phase, additional ullage must be added to accommodate the associated 6.7% solid volume expansion. By choosing the right amount of ullage, one may "dial in" the initial

porosity—a critical factor for the convective burning mechanism.

Our technique for setting the initial porosity involves calculating the containment and constituent volumes. We also measure the tube strain near both ends, by which we infer the actual tube volume and obtain a better estimate of the true porosity. While simple in principle, the methods are somewhat involved in detail. We have published these important details elsewhere [3].

The shot is mounted in an oven made of high temperature insulating material. The top and bottom wall contain radiative heating elements. The walls facing and opposite the camera have windows to observe the shot and transmit the flash light, respectively. The oven heaters are controlled by a PID temperature controller via an SCR power controller. The oven temperature ramp rate is typically 1 to 3 hours; the soak period is typically 1 to 2 hours. Type-K thermocouples are placed at various locations in and around the HE assembly to monitor the temperature during heating and soaking. At shot time, all thermocouples read the same temperature to within a few degrees Celsius.

The explosive is initiated at one end by a ceramic assembly containing a nichrome hot wire. The ignitor power is variable; however, a typical value of 50 W ignites the HE in $\sim$3 minutes or less. The camera is triggered by one of three (for redundancy) contact wires mounted near the ignition end. Experience has shown that about 1 to 1.5 mm standoff provides about the right trigger timing.

The test is backlit by two continuous 2000 W Xenon arc lamps. The tube is viewed in silhouette by a Cordin 550-62 electronic framing camera. The shot is mounted inside a walk-in firing vessel; the lights and camera are mounted

Preprint of http://dx.doi.org/10.1016/j.proci.2008.05.034

outside and access the shot via glass viewing ports. The 550-62 is a rotating mirror camera with 62 individual CCD sensors of 10-bit depth and one Mpixel resolution. The framing rate is variable from ∼12,000 to 4 Mfps. The model 550 supports pre-trigger, which we may use as desired since the lighting is continuous.

3 Experimental Observations

In this paper we describe tests at 155 C (β-phase HMX) and ∼1.3% target porosity (the nominal value for PBX 9501). This temperature was chosen because it is close to the highest value that the HE is sure to be entirely in the β-phase. The first shot (only) was illuminated by a Cordin 607 flash lamp, which has about a 100 μs delay to full light intensity. At the time of the first picture the tube radius had uniformly swelled by ∼2 mm over it's entire length—except near the ends, which were prevented from expanding by rigid constraint (Fig. 1). The deformation at this stage appeared much as if the tube was being quasi-statically pressurized.

Over an additional ∼100 μs, deformation localized in a region near the end opposite the initiation source. (A similar localization occurred in a quasi-static pre-test.) The failure location was somewhat surprising; one might have expected reaction to run away first near the initiation end. At 500 μs after the first picture, the tube began to split open at the location of the bulge. Fortuitously, the split occurred on the side facing the camera, and the light intensity of the burning HE was right to produce a good exposure. As the split continued to grow, one could see a bright horizontal band running in the axial direction, as well as two other bright spots. The bright band persists for several frames, ruling out the possibility of an artifact.

Preprint of http://dx.doi.org/10.1016/j.proci.2008.05.034

Figure 2 shows a sample frame in which the tube is splitting. Superimposed upon the photograph are the estimated locations of the charge segments prior to ignition. The bright band occurs at the pre-ignition location of the charge edge. From this we conclude that the bright band corresponds to burning on the surface of a basically intact HE slug. Note that a uniformly glowing surface-burning layer would indeed appear brightest at the charge edge, where the projected thickness is many times the actual thickness.

Figure 3 shows a photograph of the recovered shot assembly. The steel frame is intact, and the copper tube is essentially unchanged from the last dynamic picture, except that the ripped region ultimately peeled open wider—clearly under substantial force. Combustion products and unburned HE shattered the 1/8-in thick glass observation window, and unburned HE was found splattered on the vessel wall several feet away. Most of the HE remained in the tube and burned slowly over a period of 5-10 minutes.

The second shot was a repeat of the first except for lighting conditions and timing. This shot (only) used a single arc lamp, which allowed the first image to be captured without a delay relative to the touch wire trigger. The earlier pictures revealed that the tube peels away from the HE as a wave that travels at an average axial speed of $\sim$500 m/s, with an amplitude of $\sim$2 mm. The resulting bulge was fairly uniform—much like in the first test. This observation leads us to suspect that a peel-off wave likely occurred in the first test also, but that the first picture occurred too late to observe it.

Figure 4 plots the measured peel-off wave speed. This curve was obtained by differentiating an analytic fit to x-t data extracted from the high-speed pictures. The axial distance is relative to the first x-t point. The speed decreases

Preprint of http://dx.doi.org/10.1016/j.proci.2008.05.034

from an initial value of ∼800 m/s, toward what appears to be a plateau at ∼300 m/s. Propagation appears to abruptly stall near the end. The speed in Fig. 4 is plotted up to the stall point.

The peel-off wave was followed, after a ∼10 cm plateau, by a second expansion. This condition resulted in a rupture near the initiation end. A rupture near the opposite end also occurred, much like in the first test. The two ruptures closely resembled that shown in Fig. 4, and caused significantly more damage to the shot oven and peripheral hardware than did the single rupture of the first shot.

4 Steady Peel-off Wave Model

Figure 5 shows a schematic drawing of a peel-off wave, including what we conjecture to be happening on the inside. The outer case shape is the observable feature; the interior structure is inferred from supporting observations (e.g. Fig. 2) and previous experience with flames in cracked or flawed HE, e.g. [5][6][7].

Our model, based on the Fig. 5 drawing, is intended to be the simplest formulation that captures the most essential physical features. In proposing such a model we do not wish to trivialize a problem that is actually quite complex in detail. Rather, it is our hope that the successful features of this simple model will serve to motivate more realistic ones.

4.1 Material Model

The HE is assumed to be rigid; whereas, the tube is allowed to deform (stretch). The tube is assumed to stretch elastically to the yield stress, and perfectly plastically thereafter. We assume that the initial wall thickness δ_0 is small

Preprint of http://dx.doi.org/10.1016/j.proci.2008.05.034

compared to the fixed HE radius r_0 (the thin shell approximation). We further assume that the wave slope $y'[x]$—where y is the gap thickness and x is the axial distance—is everywhere small (the long-wavelength approximation). The predominate stress is then a simple hoop stress. Finally, we assume a constant wall density ρ_w, such that the cross-sectional area is conserved during stretching.

These assumptions lead to the following equations for the quasi-static (equilibrium) gas pressure P_{eq} necessary to expand the tube to a gap width y:

$$P_{eq}[y] = \begin{cases} \frac{E\,\delta_0\,y}{(r_0+y)^2}, & \text{if} \quad y < \frac{\sigma_y r_0}{E} \\ \frac{\sigma_y\,\delta_0\,r_0}{(r_0+y)^2}, & \text{if} \quad y \geq \frac{\sigma_y r_0}{E}, \end{cases} \tag{1}$$

where E and σ_y are Young's modulus and the tensile yield stress, respectively, for the tube material.

The force imbalance per unit area is $P - P_{eq}$. By Newton's law, this quantity is equal to the tube mass per unit wall area times the wall acceleration:

$$P - P_{eq}[y] = \left(\frac{r_0\,\delta_0\,\rho_w}{r_0 + y}\right)\ddot{y}, \tag{2}$$

where "dot" indicates a derivative with respect to time. Note that the wall acceleration is predominately in the radial direction since $y'[x]$ is small.

4.2 Burn Model

High explosive deflagration rates are usually measured in a *strand burner experiment* [5], wherein a bare HE stick is burned in a closed vessel. The wave progress and vessel pressure are measured to obtain the burn rate as a function of pressure. Experimentally, one finds that this relationship follows

Vielle's law:

$$\dot{m}_A = \alpha\, P^{\beta}, \tag{3}$$

where α and β are experimentally determined constants.

Equation (3) is only valid only for conductive burning. However, as the ambient pressure is increased, the flame becomes increasingly prone to "jumping" to a convective burn mode [5]. This is because pressed HE pellets (especially those with little or no binder) exhibit a degree of connected porosity. Under the right conditions, the burning can zip ahead through these porous spaces [8].

4.3 Flame Acceptance and Initial Conditions

If a flame burns on a surface containing a crack, the flame will enter and burn in the crack when its width is of order the reaction zone thickness at the ambient pressure. The critical pressure P_c above which the flame enters a gap of width y_c is approximated by *Belyaev's law* [9]:

$$P_c = \left(\frac{K}{4\, y_c^2}\right)^{\frac{1}{1+2\beta}}, \tag{4}$$

where K is an experimentally-determined constant, and β is the pressure exponent from Vielle's law. Belyaev's law is semi-empirical; the entry and propagation of a flame in a crack has not been measured or modeled in detail. In any case, the propagation of a flame into a crack is different and evidently more complicated than the classical flame quenching problem.

Berghout et. al [12] performed a calibration of Eq. (4) to PBX 9501, with good results. To use their calibration we must account for the fact that the peel-off wave gap has one burning surface; whereas, Berghout et al.'s calibration is

Preprint of http://dx.doi.org/10.1016/j.proci.2008.05.034

for cracked HE with two burning surfaces. We apply a nominal correction by interpreting y_c in Eq. (4) as the gap half-width in Belyaev's law. Although the accuracy of this simple symmetry approximation is unknown—especially in light of heat transfer to the metal wall—there is currently no basis by which to make a better estimate.

Equation (4) tells us that a flame cannot propagate down the HE/tube interface unless there is a sufficiently wide "starter" crack. In present model we assume that pre-pressurization by ignitor product gases creates, over a relatively long period of seconds to minutes, a uniform gap running the length of the tube. The peel-off wave starts when the gap width reaches criticality, determined as shown in Fig. 6. As P increases by product pressurization, y also increases according to Eq. (1), and y_c decreases according to Eq. (4). Criticality is reached where the two curves cross, which occurs at $y_c = 3\,\mu$m and $P_c = 61$ bar.

4.4 Flow Model

The peel-off wave depicted in Fig. 5 is in laboratory coordinates. For modeling purposes we prefer wave-fixed coordinates, obtained by subtracting the wave speed V from Fig. 5, and flipping the picture horizontally so that the flow moves from left to right.

In this frame the walls move at speed V. Since the flow is generated entirely by mass injection, its speed is zero at the flame front and accelerates to the ultimate speed V (corresponding to stagnation in the lab frame) at a fixed downstream location (i.e., the back boundary) in the lab frame.

We assume that the combustion product gas temperature T_p is fixed at the

adiabatic flame temperature. The physical argument for this assumption is that the flow is entirely composed of injected combustion products. Although heat loss to the copper wall is likely to be a significant factor, its consideration lies beyond the scope of a pressure-based model.

We further assume that wall ignition occurs promptly; that is, we assert that combustion starts as soon as Eq. (4) allows. This behavior represents a limiting case of what can physically happen. Clearly, actual ignition behavior must involve heat transfer effects that are neglected in this analysis. As noted in connection with flame acceptance, the lighting dynamics of flames propagating in cracked HE is an interesting unsolved problem.

We apply classical quasi-1D gasdynamic theory to a self-forming nozzle defined by the wall shape. The interesting twist on this problem is the coupling between the wall (nozzle) shape and the mass injection. The energy equation reduces to the condition $T = T_p$, leaving only the mass and momentum conservation equations. The steady mass equation is $\dot{m} = \rho\, A\, v$, where $\dot{m}$ is the total mass flowing in the annular channel, A is the total area, and v is the flow velocity. Applying all the above assumptions gives

$$a^2\, \alpha\, P^\beta = (y\, v\, P)', \tag{5}$$

where $a = \sqrt{R_p T_p}$ is the sound speed, and "prime" denotes a derivative with respect to x. Note that the specific heat ratio "γ" in the ideal gas sound speed equation is unity for the assumed isothermal flow.

The steady momentum equation is

$$\mathrm{d}(AP) + (v - V)\, \mathrm{d}\dot{m} + \dot{m}\, \mathrm{d}v = 0, \tag{6}$$

Preprint of http://dx.doi.org/10.1016/j.proci.2008.05.034

where $\mathrm{d}\dot{m}$ represents a differential increment of mass injection [10]. Equation (6) accounts for the fact that the mass-ejecting wall moves in the wave frame, and therefore adds lateral momentum (i.e., it acts as an ejector pump). Applying all the above assumptions to Eq. (6) gives:

$$(P\,y)' + \alpha(v - V)P^{\beta} + \left(\frac{y\,v\,P}{a^2}\right)v' = 0. \tag{7}$$

Equations (2), (5), and (7) provide three differential equations in the three unknowns, y, v, and P. Equation (2) must be transformed to spatial form:

$$P = \mathrm{f}[y', w]P_{eq} + \left(\frac{r_0\,\delta_0\,\rho_w V^2}{r_0 + y}\right)y''. \tag{8}$$

The function $\mathrm{f}[y', \epsilon]$ is defined as

$$\mathrm{f}[y', \epsilon] = \tanh\left[\frac{5}{2} + \frac{y'}{\epsilon}\right]. \tag{9}$$

Its sole purpose is to suppress elastic rebound of the almost perfectly plastic copper tube. The parameter ϵ is variable, and is set by trial and error to a sufficiently small value that $y[x]$ is a non-decreasing function.

The flame front sits at $y = y_c$, at which point we take $x = 0$. The flow initial conditions are $y[0] = y_c$, $y'[0] = 0$, $P[0] = P_c$, and $v[0] = 0$. The undetermined wave speed V appears in Eqs. (7) and (8). We therefore perform a shooting problem, assuming trial values of V and searching for the one that satisfies the downstream boundary condition.

As previously noted, the correct value of V would be that for which $v = V$ at the back boundary, except that for realistic model parameters the flow becomes sonic ($v = a$) well before that point. At the sonic condition the calculation

Preprint of http://dx.doi.org/10.1016/j.proci.2008.05.034

becomes singular, with v' becoming large (numerically indistinguishable from infinite) as $v \to a$. The only way to satisfy the downstream boundary condition is if $v = V$ at the sonic point. Thus $V = a$, the sound speed of the hot injected product gas.

Transforming back the lab frame, the peel-off wave propagates by the forward jetting of product gas in a small isolated region. There is no flow ahead of the jet, and there is no axial flow behind the jet; that is, injected gas flows only in the lateral direction.

4.5 Model Behavior

We now demonstrate the model behavior for the PBX 9501 parameters listed in Table 1. All numbers are published values except for α and σ_y, which have been adjusted to optimally fit the data. In both cases, the resulting values fall within the substantial variation in published values.

The model wave speed is 810 m/s, which is very close to the measured velocity near the start (Fig. 4). The model gap width, pressure, and flow velocity are plotted in Figs. 7-9. All plots are for wave-fixed coordinates, with the axial distance x starting at the flame front and increasing in the streamwise direction.

The predicted gap width (Fig. 7) increases from zero to 2 mm over a distance of 50 mm. There is a plateau for the next 100 mm, followed by a secondary expansion. The origin of this behavior is best understood by examining the pressure response (Fig. 8).

For a brief time, inertial confinement renders the wall immobile. This transient rigidity causes the pressure to spike. As the wall gains speed in response to the

Preprint of http://dx.doi.org/10.1016/j.proci.2008.05.034

high gas pressure, the channel widens and the pressure rapidly drops. Because the wall has accrued momentum, the wall overshoots its equilibrium position, such that P falls below P_{eq}. Soon the wall comes to rest, corresponding to the plateau in Fig. 7. The response to this point is somewhat reminiscent of an exploding popcorn kernel.

Meanwhile the HE continues to burn, causing the pressure to re-build until the applied pressure exceeds the case resistance. This marks the beginning of a gentler but larger secondary expansion. If the solution is carried out further, the tube continues to "ratchet ring" in this manner.

Figure 9 shows how the flow speed goes from zero-to-sonic in 100 μm, at which point it stagnates in the lab frame. The flow structure is more easily visualized by transforming Fig. 9 back to the lab frame, yielding Fig. 10. The coordinate X increases in the direction of wave propagation. This "encapsulated" jet structure propagates to the right at speed $V = a$.

Figure 11 shows a high-speed photograph of the measured tube profile, with the calculated peel-off wave (red curves) superimposed. Because of the small peel-off wave amplitude, the picture has been expanded 3× in the vertical direction for easier viewing. The agreement is surprisingly good.

5 Discussion

Our peel-off model predicts that a supercritical starter crack is necessary for a peel-off wave to propagate. However, it might not be necessary for the starter crack to run the entire tube length for the wave to do so. This would be the case if, once a peel-off wave becomes established, stress waves running ahead in the high sound speed metal tube dynamically open a crack just ahead of

the flame front. That mechanism is not captured in our simple stress model, and our observations to date are not suggestive of such behavior.

It seems more likely that the initial starter crack will generally extend only part way down the tube, and that the peel-off wave will indeed stall where $y < y_c$. At this point the HE behind the stalled peel-off wave head continues to burn. If the tube has not yet ruptured, HE products will evidently create a new starter crack, in much the same way that the ignitor gases did initially. This scenario would cause peel-off to pulsate until confinement fails. Our observations to date only hint at this behavior, but it is a phenomenon worth pursuing in the future.

We have previously described results at 175 C (δ-phase HMX) and 1.3% target porosity [4]. This temperature was chosen because it is close to the lowest value at which the HE reliably transitions to the δ-phase given sufficient time. In [4], we analyzed a quasi-steady deflagration wave that traveled down the tube at a steady speed of 550 m/s, causing the tube to bell out in a trumpet shape in a manner reminiscent of a DTCT.

Because this more vigorous burning mode nevertheless propagated at the same speed as a peel-off wave, and also because it is prone to stalling in the same way, we conjectured that this behavior is also peel-off wave triggered. We further proposed that the pressure spike associated with the peel off wave (Fig. 8) initiates convective burning in the more porous δ-phase material. Independent of these assumptions, we showed that the generated flow was a burning two-phase mixture.

Two additional δ-phase tests at other initial conditions have exhibited the

Preprint of http://dx.doi.org/10.1016/j.proci.2008.05.034

same general type of behavior, and all have stalled part way down the tube. In contrast to pure peel-off waves, peel-off convective waves leave unburned HE in the tube after they fail. This counterintuitive behavior evidently occurs because the tube has ripped wide open when the wave fails; whereas, for a pure peel-off wave the tube remains sealed until all the HE is ignited.

A sixth test, with nominally identical conditions to the 175 C peel-off convective wave described above, transitioned to detonation about 2/3 of the way down the tube. Although the camera malfunctioned, some information was gained from the fact that copper strips were welded to the support rods. This indicated that the behavior was much more vigorous from the start. Damage to the rods abruptly increased at the DDT point [4]. It would appear that DDT is the exception rather than the rule, at this level of confinement. Increasing the confinement will presumably lead to more vigourous burning and more consistent DDT events.

6 Conclusions

Deflagration cylinder test experiments were performed on PBX 9501 at 155 C initial temperature and ∼1.3% porosity. These experiments revealed a previously unidentified thermal explosion mode, whereby the tube peeled away from the HE as a wave that traveled at ∼500 m/s. Although the observed wave decelerated, a simple, steady model of the phenomena captures the essential observed features. Other interesting phenomena observed by the DFCT, including DDT, are reported elsewhere [4].

The likely reason that peel-off waves have not been observed is that photographic studies of cookoff case failure are rare. They may in fact comprise

a common failure mode in HE systems with moderate ductile confinement—both in their pure form, and as the lead disturbance in the more vigorous peel-off convective waves. If so, it is important to understand this response and its relation to the greater HE thermal safety problem.

Acknowledgements

The DFCT was conceived by Blaine Asay and Guillermo Terrones. The project leader was Pete Pittman. Bill Santistevan performed detailed design of the shot assembly. Brent Faulkner, Bob Mier, and Larry Vaughan provided shot assembly/fielding support. Blaine Asay, Bryan Henson, and Laura Smilowitz consulted on various experimental details. This project was funded by the U.S. Department of Energy.

References

[1] J.F. Wardell, J.L. Maienschein, in: *11th Symp. on Detonation*, ONR, 1998, pp. 384-393.

[2] F. Leuret, F. Chaissé, H. N. Presles, B. Veyssière, in: *11th Symp. on Detonation*, ONR, 1998, pp. 693-700.

[3] S.I. Jackson, L.G. Hill, L.L. Davis, J.S. Morris, in: *Proc. 24th Propulsion Hazards Subcommittee Meeting*, JANNAF, 2008.

[4] L.G. Hill, J.S. Morris, S.I. Jackson, in: *Proc. 24th Propulsion Hazards Subcommittee Meeting*, JANNAF, 2008.

[5] J. L. Maienschein, J. B. Chandler, in: *11th Symp. on Detonation*, ONR, 1998, pp. 872-879.

[6] P.M. Dickson, B.W. Asay, B.F. Henson, L.B. Smilowitz, *Proc. R. Soc. Lond. A* 460 (2004) 3447-3455.

[7] H.L. Berghout, S.F. Son, L.G. Hill, B.W. Asay, *J. Appl. Phys.* 99(11) (2006) 114901-114907.

[8] L.G. Hill, in: *14th APS Topical Conference on Shock Waves in Condensed Matter*, APS, 2005, pp. 531-534.

[9] H.H. Bradley, T.L. Boggs, Convective Burning in Propellant Defects: a Literature Review, *Naval Weapons Center, China Lake, CA Report No. NWC-TP-6007*, 1978.

[10] M.J. Zucrow, J.D. Hoffman, *Gas Dynamics*, John Wiley & Sons, New York, NY, 1976.

[11] M.J. Ward, S.F. Son, M.Q. Brewster, *Combustion and Flame* 114 (1998) 556-568.

[12] H.L. Berghout, S.F. Son, D.B. Skidmore, D.J. Idar, B.W. Asay, Thermochimica Acta (384) (2002), 261-277

[13] W. Bolton, CRC Engineering Materials Pocket Book, CRC Press, Boca Raton, FL (1989)

[14] G.R. Parker, B.W. Asay, P.M. Dickson, B.F. Henson, L.B. Smilowitz, in: *13th APS Topical Conference on Shock Waves in Condensed Matter*, PAS, 2003, pp. 1009-1012.

[15] G.R. Parker, B.W. Asay, P.M. Dickson, P. Rae, A. Ionita, in: *15th APS Topical Conference on Shock Waves in Condensed Matter*, APS, 2007.

Preprint of http://dx.doi.org/10.1016/j.proci.2008.05.034

Tables

Table 1
Peel-off Wave Model Parameters

Symbol	Value	Unit	Ref.
T_p	2700	K	[11]
R_p	243	J/(kg-K)	[11]
α	9×10^{-5}	s/m, $\beta = 1$	cf. [11][12]
β	0.92	—	[12]
σ_y	250	MPa	cf. [13]
K	8×10^8	$\mathrm{kg}^3/(\mathrm{m\text{-}s}^6)$, $\beta = 1$	[12]

List of Figures

Preprint of http://dx.doi.org/10.1016/j.proci.2008.05.034

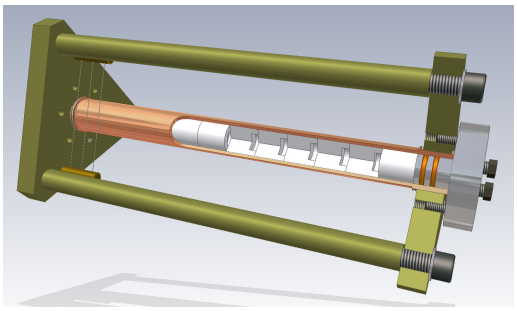

Fig. 1. Schematic diagram of the deflagrating cylinder test.

Preprint of http://dx.doi.org/10.1016/j.proci.2008.05.034

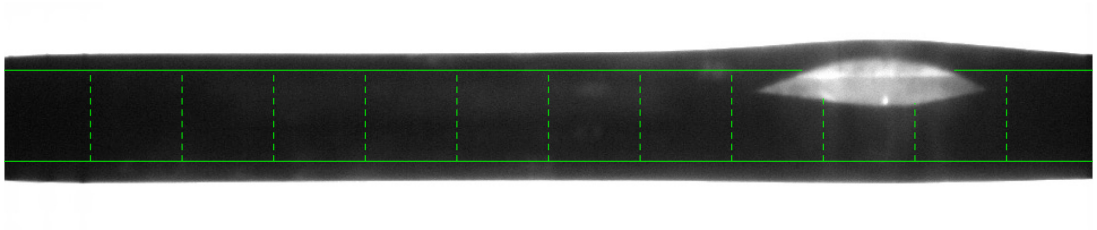

Fig. 2. High speed photo of the tube splitting. The bright line on the HE suggests that reaction occurs only at the surface.

Preprint of http://dx.doi.org/10.1016/j.proci.2008.05.034

Fig. 3. Photo of a recovered shot assembly (Shot# 8-1032).

Preprint of http://dx.doi.org/10.1016/j.proci.2008.05.034

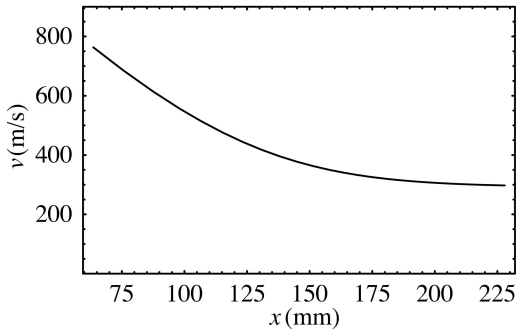

Fig. 4. Measured peel-off wave speed (Shot# 8-1044).

Preprint of http://dx.doi.org/10.1016/j.proci.2008.05.034

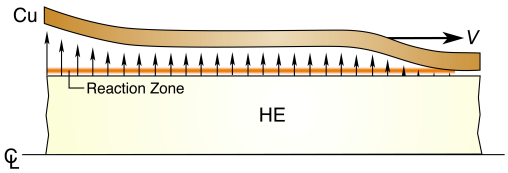

Fig. 5. Schematic diagram of a peel-off wave.

Preprint of http://dx.doi.org/10.1016/j.proci.2008.05.034

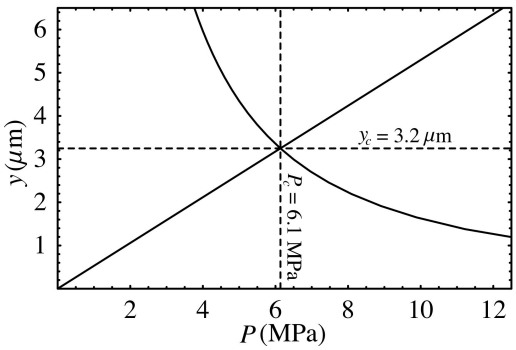

Fig. 6. Initial condition: critical pressure and gap width.

Preprint of http://dx.doi.org/10.1016/j.proci.2008.05.034

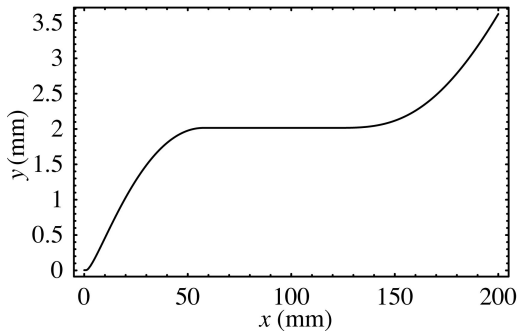

Fig. 7. Calculated gap width vs. axial distance (wave frame).

Preprint of http://dx.doi.org/10.1016/j.proci.2008.05.034

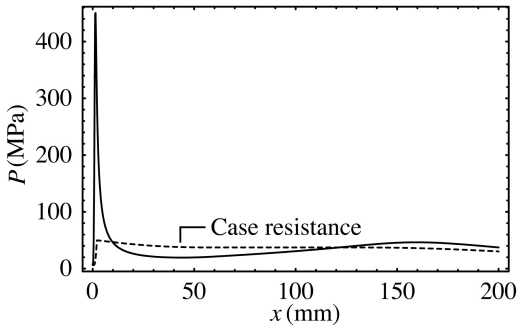

Fig. 8. Calculated pressure vs. axial distance (wave frame).

Preprint of http://dx.doi.org/10.1016/j.proci.2008.05.034

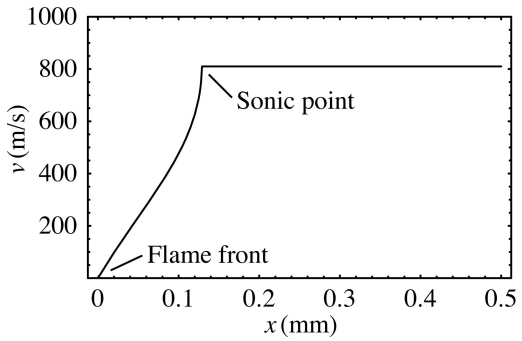

Fig. 9. Calculated speed vs. axial distance (wave frame).

Preprint of http://dx.doi.org/10.1016/j.proci.2008.05.034

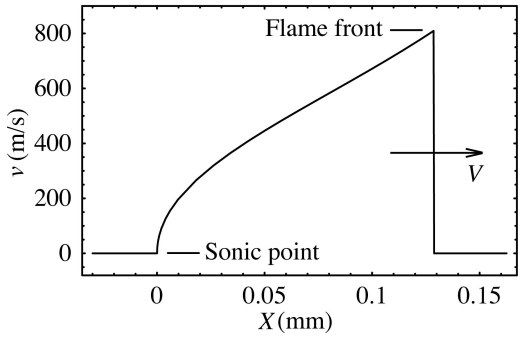

Fig. 10. Calculated speed vs. axial distance (lab frame).

Preprint of http://dx.doi.org/10.1016/j.proci.2008.05.034

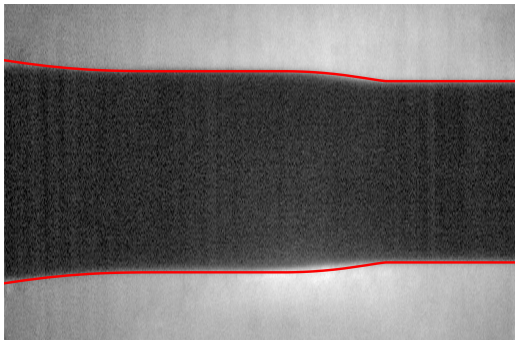

Fig. 11. Experimental vs. calculated tube shape. The picture is expanded 3× in the vertical direction for clarity.